Research Article

Chip Thickness and Microhardness Prediction Models during Turning of Medium Carbon Steel

S. A. Alrabii and L. Y. Zumot

Recommended by Ibrahim Sadek

Cutting tests were conducted to medium carbon steel using HSS tools with cutting fluid. The experimental design used was based on response surface methodology (RSM) using a central composite design. Chips were collected at different machining conditions and thickness and microhardness measurements taken and analyzed using "DESIGN EXPERT 7" experimental design software. Mathematical models of the responses (thickness and microhardness) as functions of the conditions (speed, feed, and depth of cut) were obtained and studied. The resultant second-order models show chip thickness increases when increasing feed and speed, while increasing depth of cut resulted in a little effect on chip thickness. Chip microhardness increases with increasing depth of cut. It also increases with increasing speed and feed up to a certain level beyond which further increases cause a drop in microhardness.

1. Introduction

Material removal processes are an integral part of many manufacturing processes. It is important to study the many factors influencing these operations in order to achieve better performance and economy. The chip formation process occurring during metal cutting is a complicated one, involving plastic deformation, work hardening, heat generation, and tool wear. Finding a range of cutting conditions that will give maximum efficiency can help manufacturers produce more economically.

High-speed steel (HSS) cutting tools are greatly needed in industry to machine carbon steels due to their strength and toughness properties. To optimize their use, it is essential to control and properly select the cutting conditions applied in cutting operations

Table 2.1. Hardness values at different radii for work material cross-section.

Number	Location (mm from center)	HRB
1	25 (edge)	92.9
2	17.5	91.1
3	10	90.8
4	5	92.5
5	0 (center)	86.6

to obtain higher material removal rate and proper type of chip for higher machinability. Therefore, chip thickness and microhardness are considered significantly important for evaluating productivity of any cutting operation leading to the need to formulate prediction models for chip thickness and microhardness as functions of operating conditions.

The use of response surface methodology (RSM) helps reduce the number of tests required to achieve a statistically sound result. RSM aims at producing a surface prediction model for multiple parameters [1]. The methodology has been used to analyze and predict shear flow stress when using HSS tools in turning of mild steel [2]. It has also been used in tool life testing and producing prediction models for tool life and material removal rates as functions of machining parameters [3–5]. Furthermore, most of the research work in turning operations using RSM or factorial designs has been directed at the analysis and prediction of surface roughness, or surface finish as a function of both machining parameters and/or use of different coated tools [6–12]. However, little work on the machining of steels has been given to the prediction of chip thickness and/or microhardness [13].

The aim of this paper is to study the effect of varying machining parameters on chip thickness and microhardness during longitudinal turning of medium carbon steel using HSS tools and cutting fluid, in order to develop prediction models for these by using response surface methodology. The machining parameters studied are speed (v), feed (f), and depth of cut (d). The software DESIGN EXPERT 7 was used to develop the RSM model. Results of test runs are reported, as well as the prediction models produced within a 95% confidence interval.

2. Work material preparation

The material used was 1055 steel (carbon percent 0.55%). Bars of 50 mm diameter and 1-meter length were used. To investigate the variation of hardness values in the sample from which deductions can be made regarding level of coring in the sample, the Rockwell hardness (HRB) of the work material was measured at different radii using the Rockwell hardness testing machine.

Five measurements at 5–7.5 mm intervals starting near the edge and moving towards the center were made. The Rockwell B scale was used at 100 Kgf load. Results showed the material to have a hardness of (HRB 91) on average (see Table 2.1, Figure 2.1), and that no coring existed.
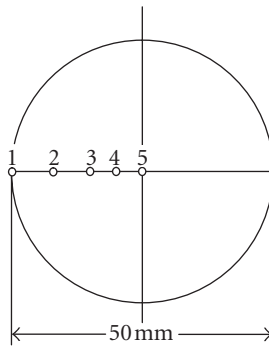
FIGURE 2.1. Locations of hardness tests at different radii of the work material cross-section.

3. Cutting tool preparation

HSS cutting tools with 5% cobalt (M-grade SI 6) were used with specific cutting angles, such that the tools cut orthogonally. This meant a back rake angle (α_b), side rake angle (α_s), and side cutting angle (Ψ) of zero degrees, resulting in a rake angle (α) of zero degrees as well as high relief angles. The tool signature is listed below (**Figure 3.1** illustrates the tool geometry):

  (i) α_b: back rake angle = 0°;
 (ii) α_s: side rake angle = 0°;
(iii) ERA: end relief angle = 16°;
 (iv) SRA: side relief angle = 21.5°;
  (v) ECEA: end cutting edge angle = 23°;
 (vi) Ψ: side cutting edge angle = 0°;
(vii) NR: nose radius = 0.25 mm.

4. Experimental design and testing

The experimental design used was the response surface methodology using a central composite rotatable design for 2^3 factors, with 5 central points and $\alpha = \pm 2$. 19 tests were performed according to the experimental design matrix (*5 centre points*). The tests were performed at random using the run order listed in Table 4.1. The parameters were chosen such that they take into consideration the limitations of the machine and in order to avoid excessive chatter. Each parameter was tested at different code levels of -2, -1, 0, $+1$, and $+2$, whereby each level tested conformed to an actual value equivalent to the coded value.

The machine used to perform the cutting tests was a Bulgarian SLIVEN 400 Turning Machine. The work material bars were cut in a longitudinal turning operation using cutting fluid for at least 10 minutes per test to ensure stable chip thickness measurements. Chips were collected after 10 minutes of cutting to ensure stability of chip thickness. Since cutting tests were performed with speed kept constant, variations in diameter of work piece were taken into account when selecting the RPM at which turning took place.
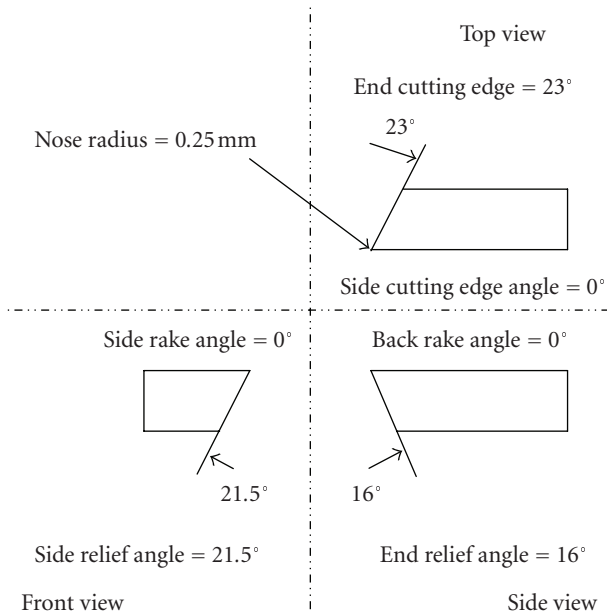
FIGURE 3.1. Cutting tool geometry.

5. Chip thickness and chip microhardness measurement

At the end of each test, the weight (M_c) and length (L_c) of 5 collected chips were measured using a calibrated weight balance and a measuring length vernier, respectively. The average chip thickness was then obtained as per [14]

$$t_c = \frac{M_c \cos \psi}{L_c w \rho} \times 10^3, \tag{5.1}$$

where (M_c) is the chip specimen mass in grams, (L_c) is the length of the chip sample in mm, (ρ) is the density of the work material in g/cm³ (7.87 g/cm³), (w) is the width of the chip taken as the depth of cut used in mm, and (ψ) is the primary (side) cutting edge angle.

Chips were collected randomly at the end of each cutting test in order to measure the microhardness of the chip. Specimens were mounted, ground, and polished on a grinding and polishing apparatus to obtain a clean, smooth chip surface suitable for the microhardness measurement test. At least 3 measurements of microhardness were taken at the surface of different chips on the mount.

The Vickers microhardness tester was used for these measurements. With the average of these measurements, the Vickers hardness number (VHN) of these chips was calculated using (5.2) [15]. The load used on the Vickers testing machine was 5 Kgf:

$$\text{HV} = \frac{1.854P}{L^2}, \tag{5.2}$$

TABLE 4.1. Experimental design matrix used.

Test	Run	Speed, v (code A) (m/min)		Feed, f (code B) (mm/rev)		Depth of cut, d (code C) (mm)	
		Coded	Value	Coded	Value	Coded	Value
1	11	−1	20	−1	0.3	−1	0.25
2	8	1	40	−1	0.3	−1	0.25
3	6	−1	20	1	0.5	−1	0.25
4	17	1	40	1	0.5	−1	0.25
5	10	−1	20	−1	0.3	1	0.5
6	19	1	40	−1	0.3	1	0.5
7	1	−1	20	1	0.5	1	0.5
8	5	1	40	1	0.5	1	0.5
9	2	−2	10	0	0.4	0	0.375
10	15	2	50	0	0.4	0	0.375
11	9	0	30	−2	0.2	0	0.375
12	7	0	30	2	0.6	0	0.375
13	12	0	30	0	0.4	−2	0.125
14	3	0	30	0	0.4	2	0.625
15	4	0	30	0	0.4	0	0.375
16	13	0	30	0	0.4	0	0.375
17	14	0	30	0	0.4	0	0.375
18	16	0	30	0	0.4	0	0.375
19	18	0	30	0	0.4	0	0.375

where (P) is the load used applied for 10 seconds, and (L) is the arithmetic mean of the diagonal indentations $d1$ and $d2$ made by the indenter on the work material.

The average results of the measurements obtained are shown in Table 5.1 for each test. Also, the typical values of M_c, L_c, and w for one test (run 13) are given in Table 5.2.

6. Results and discussion

The average responses obtained for thickness and microhardness were used in calculating the models of the response surface per response using the least-squares method.

For chip thickness prediction, a reduced cubic model in coded terms was analyzed with backwards elimination of insignificant coefficients at an exit threshold of alpha = 0.1. Some coefficients were removed and reinstated in order to preserve hierarchy and allow for obtaining a formula with actual factors rather than coded ones. The terms removed were BC, AB^2, AB, B^2, C, AC, C^2, ABC, A^{2}C. The terms that were reinstated were AB. This means that depth of cut had no significant effect on chip thickness values.

Table 6.1 shows analysis of variance produced by the software for the remaining terms. The model is significant at 90% confidence. It is noted that the interaction between speed

TABLE 5.1. Average results of thickness and VHN/5/10 measurements per test.

Test	Run	v	f	d	VHN	t_c (mm)
1	11	20	0.30	0.250	350.3014	0.994273
2	8	40	0.30	0.250	355.0106	1.182254
3	6	20	0.50	0.250	321.949	0.514471
4	17	40	0.50	0.250	361.8089	1.261542
5	10	20	0.30	0.500	387.5238	0.636477
6	19	40	0.30	0.500	384.2923	1.001228
7	1	20	0.50	0.500	346.3279	0.609596
8	5	40	0.50	0.500	373.8599	0.549657
9	2	10	0.40	0.375	309.4837	0.135257
10	15	50	0.40	0.375	362.5482	0.67777
11	9	30	0.20	0.375	305.7518	0.560848
12	7	30	0.60	0.375	374.6204	1.433699
13	12	30	0.40	0.125	377.514	0.504901
14	3	30	0.40	0.625	381.7663	0.809857
15	4	30	0.40	0.375	326.532	0.388664
16	13	30	0.40	0.375	315.4095	0.703261
17	14	30	0.40	0.375	366.7723	0.816765
18	16	30	0.40	0.375	369.2855	1.363499
19	18	30	0.40	0.375	375.3487	1.165174

TABLE 5.2. Example of calculations made for deducing average chip thickness of test 16 (run 13).

Test	Run	Chip number	L_c (mm)	M_c (gm)	w (mm)	t_c (mm)
16	1	1	5.3	13	0.375	0.831115693
16	2	2	5	11	0.375	0.745446845
16	3	3	5.2	10	0.375	0.651614375
16	4	4	3.6	7	0.375	0.658854534
16	5	5	7	13	0.375	0.62927331

and feed is insignificant while the independent effects of speed and feed as well as the interaction between squared speed and feed are also signficant. The lack of fit test indicates a good model. The final model in coded and actual terms is illustrated in Table 6.2 showing feed to have the highest impact on chip thickness.

Looking at the normal probability plot (Figure 6.1) or the chip thickness data, the residuals generally that falling on a straight line implying errors are normally distributed. Also, according to Figure 6.2 that shows the residuals versus predicted responses for chip thickness data, it is seen that no obvious patterns or unusual structure implying models are accurate.

Similarly for microhardness measurements, a reduced cubic model in coded terms was analyzed with backwards elimination of insignificant coefficients at an exit threshold of

TABLE 6.1. ANOVA for response surface reduced cubic chip thickness model.

	Sum of squares	df	Mean square	F value	p-value prob > F
Model	1.13252	5	0.226504	2.574113	0.0788
A-speed (v)	0.337819	1	0.337819	3.83916	0.0719
B-feed (f)	0.380934	1	0.380934	4.32914	0.0578
AB	0.002258	1	0.002258	0.02566	0.8752
A^2	0.314936	1	0.314936	3.579103	0.0810
A^2B	0.430555	1	0.430555	4.893053	0.0455
Residual	1.14391	13	0.087993	—	—
Lack of fit	0.552447	9	0.061383	0.415127	0.8742
Pure error	0.591463	4	0.147866	—	—
Cor total	2.27643	18	—	—	—
	Std. dev.	0.296636	R-squared	0.497498	
	Mean	0.805747	Adj R-squared	0.304229	
	C.V.%	36.81506	Pred R-squared	0.13363	
	PRESS	1.972231	Adeq precision	6.9761	

TABLE 6.2. Final equation for chip thickness in terms of coded and actual factors.

Coded chip thickness (Tc) =	Actual chip thickness (Tc) =
0.897504	10.62068
+0.145306 A	−0.71421 v
+0.218213 B	−27.8494 f
+0.0168 AB	+1.9853 vf
−0.10896 A^2	+0.012034 v^2
−0.32808 A^2B	−0.03281 v^2f

alpha = 0.1, followed by a manual elimination of some variables in order to achieve a significant model at 95% confidence. After examination of analysis results, test 14 or run 3 (code 0, 0, 2) was ignored in the run in order to achieve a robust model and the analysis performed again.

The terms removed were ABC, A^2C, AC, AB^2, B^2, BC, A^2, and AB, the terms that were reinstated were AB, and A^2.

Table 6.3 shows that the model is significant at 95% confidence and that speed, feed, and depth of cut are significant factors but the interaction of speed with feed as well as the square of speed are not, yet squared depth of cut is. The lack of fit test indicates a good model. The final model in coded and actual terms is depicted in Table 6.4 showing feed and squared depth of cut to have the highest impact on chip thickness.

Figure 6.3 shows the contour graph of speed versus feed with chip thickness as a response. Since depth of cut had no significant effect on chip thickness, only the two-factor
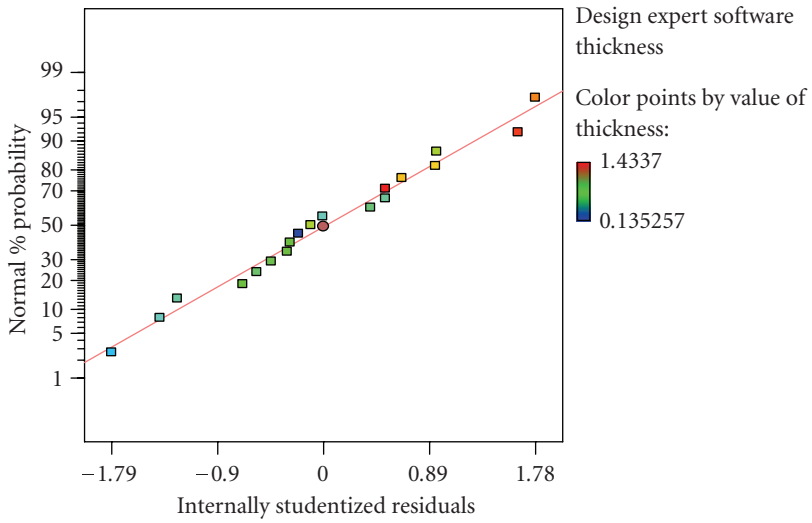
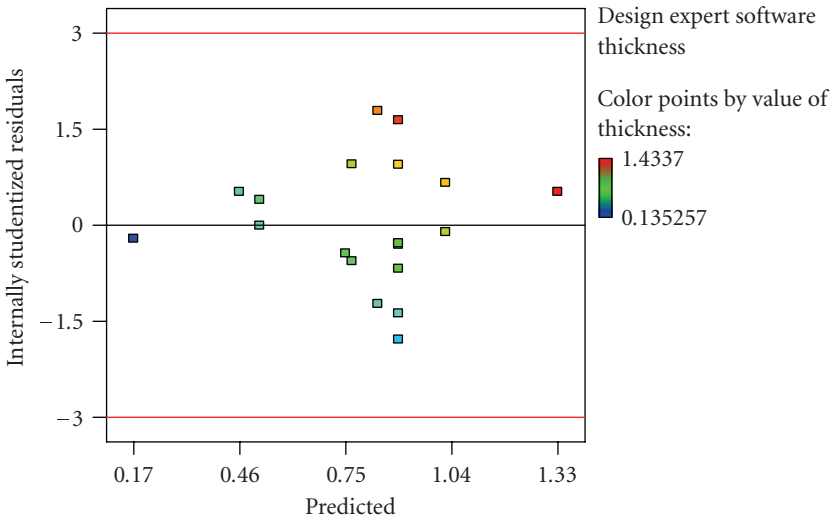FIGURE 6.1. Normal probability plot of residuals for chip thickness data.

FIGURE 6.2. Residual versus predicted response for chip thickness data.

interaction is shown. It is noted that the increase in speed leads to an increase in chip thickness at feeds of 0.3 till 0.4, while at feeds of 0.45 or more increases in speed up to (33 m/s) resulted in increases in chip thickness but beyond that, the chip thickness decreases. Increases in both speed and feed resulted in increases in chip thickness, but increases of feed at lower speeds of (20 m/s) resulted in slightly lesser thickness.

TABLE 6.3. ANOVA for response surface reduced cubic chip microhardness model.

	Sum of squares	df	Mean square	F value	p-value prob > F
Model	8592.396	7	1227.485	3.548601	0.0348
A-speed (v)	1914.032	1	1914.032	5.533376	0.0405
B-feed (f)	2371.444	1	2371.444	6.855732	0.0257
C-depth of cut (d)	1562.911	1	1562.911	4.518302	0.0595
AB	543.0868	1	543.0868	1.570038	0.2387
A^2	204.6711	1	204.6711	0.591694	0.4595
C^2	2473.485	1	2473.485	7.150728	0.0233
A^2B	2780.44	1	2780.44	8.04	0.0177
Residual	3459.068	10	345.9068	—	—
Lack of fit	418.2655	6	69.71091	0.091701	0.9936
Pure error	3040.802	4	760.2005	—	—
Cor total	12051.46	17	—	—	—
	Std. dev.	18.59857	R-squared	0.712975	
	Mean	353.5744	Adj R-squared	0.512058	
	C.V.%	5.260156	Pred R-squared	0.472845	
	PRESS	6352.984	Adeq precision	5.719197	

TABLE 6.4. Final equation for microhardness in terms of coded and actual factors.

Coded microhardness (VHN) =	Actual microhardness (VHN) =
348.0446	1357.776056
+10.93741 A	−63.77080678 v
+17.21716 B	−2447.854259 f
+13.19075 C	−580.2372968 d
+8.239287 AB	166.4291015 vf
−2.8451 A^2	1.026147219 v^2
+14.28674 C^2	914.3511032 d^2
−26.365 A^2B	−2.636496902 v^2f

Figures 6.4–6.6 show three-dimensional graphs of microhardness as a function of speed and feed at different depth of cut levels. The first noted effect is that increases in depth of cut caused increases in microhardness levels regardless of speed or feed. This increase is more pronounced at depth of 0.5 mm (Figure 6.6).

These figures also reveal that increases of speed from 20 to 30 m/s at lower feed rates of 0.4 mm/s cause a slight dercrease in microhardness but beyond that they cause an increase. However, increases in speed from 20 to 30 m/s at higher feed rates of (0.5 mm/s) cause an increase in microhardness, but increases of speed beyond that to (40 m/s) cause a decrease in microhardness.
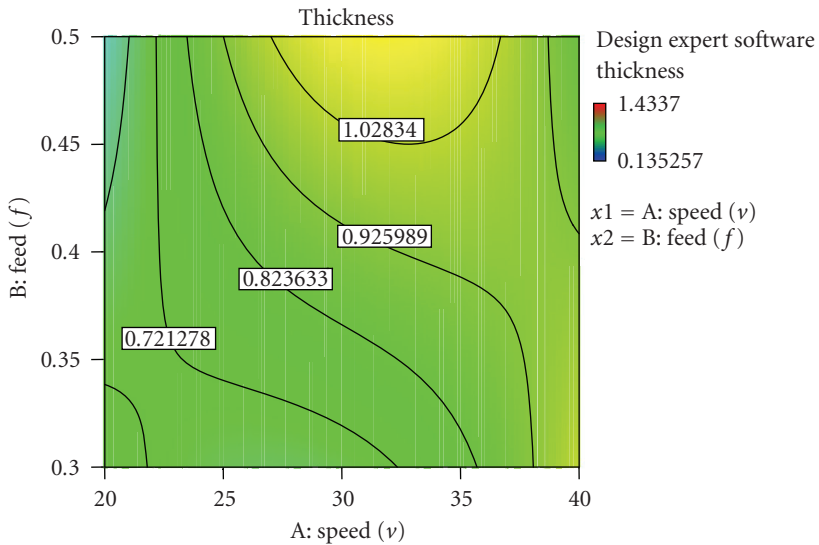
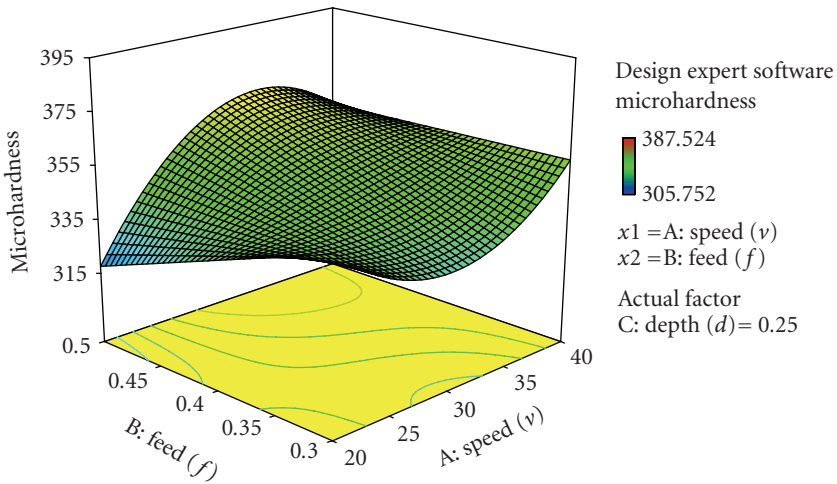Figure 6.3. Contour graph of chip thickness as a function of speed and feed.

Figure 6.4. 3D graph of microhardness as a function of speed and feed at low depth of cut ($d = 0.25$).

7. Conclusions

Second-order equations for chip thickness and microhardness as a function of speed, feed, and depth of cut were developed at 90% and 95% confidence, respectively. The chip thickness equation shows that depth of cut has no effect on chip thickness, but that increases in speed of cut and the interaction between feed and speed of cut have the greatest impact in increasing chip thickness since higher material removal rates ensue. The
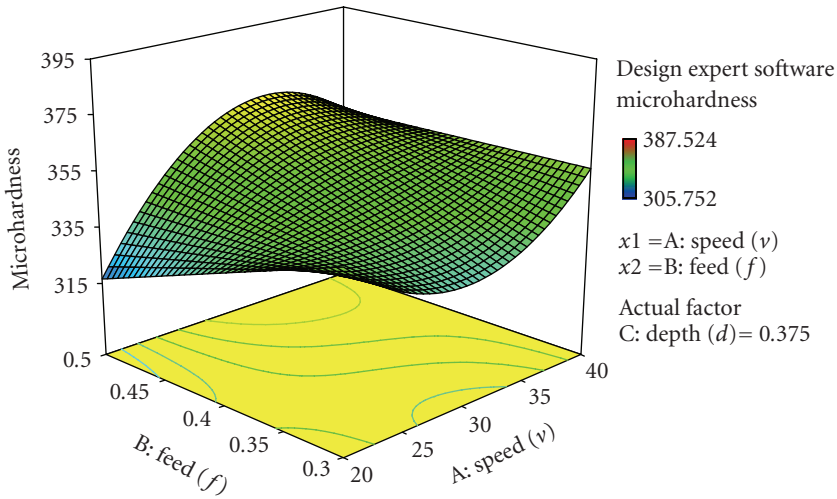
FIGURE 6.5. 3D graph of microhardness as a function of speed and feed at mid depth of cut (d = 0.375).
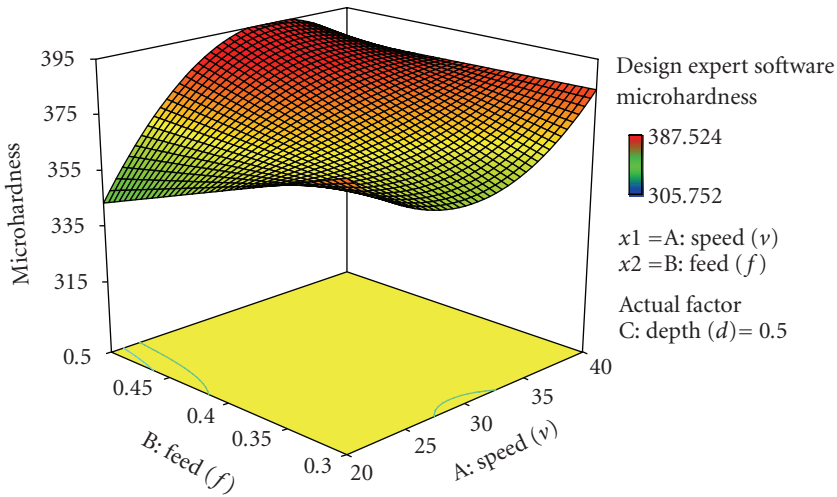

FIGURE 6.6. 3D graph of microhardness as a function of speed and feed at higher depth of cut (d = 0.5).

microhardness equation shows that increases in depth of cut have the greatest influence in increasing microhardness of chips, while increase of speed up to 30 m/s caused either an increase in chip microhardness at higher feed rates of 0.5 mm/s, yet caused a decrease at lower feed rates of 0.3 mm/s. The opposite is true for increases beyond 30 m/s, where microhardness of resultant chips increased at lower feed rates, but decreased at higher feed rates.

References

[1] D. C. Montgomery, *Design and Analysis of Experiments*, John Wiley & Sons, New York, NY, USA, 5th edition, 2001.

[2] V. K. Jain and B. K. Gupta, "Effects of accelerated tests on shear flow stress in machining," *Journal of Engineering for Industry*, vol. 109, no. 3, pp. 206–212, 1987.

[3] S. M. Wu, "Tool life testing by response surface methodology—part I and part II," *Journal of Engineering for Industry*, vol. 86, pp. 105–116, 1964.

[4] I. A. Choudhury and M. A. El-Baradie, "Tool-life prediction model by design of experiments for turning high strength steel (290 BHN)," *Journal of Materials Processing Technology*, vol. 77, no. 1–3, pp. 319–326, 1998.

[5] S. K. Choudhury and I. V. K. Appa Rao, "Optimization of cutting parameters for maximizing tool life," *International Journal of Machine Tools and Manufacture*, vol. 39, no. 2, pp. 343–353, 1999.

[6] R. M. Sundaram and B. K. Lambert, "Mathematical models to predict surface finish in fine turning of steel—part I," *International Journal of Production Research*, vol. 19, no. 5, pp. 547–556, 1981.

[7] R. M. Sundaram and B. K. Lambert, "Mathematical models to predict surface finish in fine turning of steel—part II," *International Journal of Production Research*, vol. 19, no. 5, pp. 557–564, 1981.

[8] G. C. Onwubolu, "A note on "surface roughness prediction model in machining of carbon steel by PVD coated cutting tools"," *American Journal of Applied Sciences*, vol. 2, no. 6, pp. 1109–1112, 2005.

[9] I. A. Choudhury and M. A. El-Baradie, "Surface roughness prediction in the turning of high-strength steel by factorial design of experiments," *Journal of Materials Processing Technology*, vol. 67, no. 1–3, pp. 55–61, 1997.

[10] C. X. Feng, "An experimental study of the impact of turning parameters on surface roughness," in *Proceedings of the Industrial Engineering Research Conference*, Dallas, Tex, USA, May 2001, paper no. 2036.

[11] J. P. Davim, "A note on the determination of optimal cutting conditions for surface finish obtained in turning using design of experiments," *Journal of Materials Processing Technology*, vol. 116, no. 2-3, pp. 305–308, 2001.

[12] M. Y. Noordin, V. C. Venkatesh, S. Sharif, S. Elting, and A. Abdullah, "Application of response surface methodology in describing the performance of coated carbide tools when turning AISI 1045 steel," *Journal of Materials Processing Technology*, vol. 145, no. 1, pp. 46–58, 2004.

[13] V. K. Jain, S. Kumar, and G. K. Lal, "Effects of machining parameters on the micro-hardness of chips," *Journal of Engineering for Industry*, vol. 111, no. 3, pp. 220–228, 1989.

[14] B. H. Amstead, P. F. Ostwald, and M. L. Begeman, *Manufacturing Processes*, John Wiley & Sons, New York, NY, USA, 1987.

[15] S. Kalpakjian, *Manufacturing Processes for Engineering Materials*, Addison-Wesley, Menlo Park, Calif, USA, 3rd edition, 1997.

S. A. Alrabii: Department of Mechanical & Industrial Engineering, Applied Science University, P.O. Box 926296, Shafa-Badran, Amman 11931, Jordan
Email address: alrabii@asu.edu.jo

L. Y. Zumot: P.O. Box 830342, Amman 11183, Jordan
Email address: laithzumot@hotmail.com

Special Issue on
Boundary Value Problems on Time Scales

Call for Papers

The study of dynamic equations on a time scale goes back to its founder Stefan Hilger (1988), and is a new area of still fairly theoretical exploration in mathematics. Motivating the subject is the notion that dynamic equations on time scales can build bridges between continuous and discrete mathematics; moreover, it often revels the reasons for the discrepancies between two theories.

In recent years, the study of dynamic equations has led to several important applications, for example, in the study of insect population models, neural network, heat transfer, and epidemic models. This special issue will contain new researches and survey articles on Boundary Value Problems on Time Scales. In particular, it will focus on the following topics:

- Existence, uniqueness, and multiplicity of solutions
- Comparison principles
- Variational methods
- Mathematical models
- Biological and medical applications
- Numerical and simulation applications

Before submission authors should carefully read over the journal's Author Guidelines, which are located at http://www.hindawi.com/journals/ade/guidelines.html. Authors should follow the Advances in Difference Equations manuscript format described at the journal site http://www.hindawi.com/journals/ade/. Articles published in this Special Issue shall be subject to a reduced Article Processing Charge of €200 per article. Prospective authors should submit an electronic copy of their complete manuscript through the journal Manuscript Tracking System at http://mts.hindawi.com/ according to the following timetable:

Manuscript Due	April 1, 2009
First Round of Reviews	July 1, 2009
Publication Date	October 1, 2009

Lead Guest Editor

Alberto Cabada, Departamento de Análise Matemática, Universidade de Santiago de Compostela, 15782 Santiago de Compostela, Spain; alberto.cabada@usc.es

Guest Editor

Victoria Otero-Espinar, Departamento de Análise Matemática, Universidade de Santiago de Compostela, 15782 Santiago de Compostela, Spain; mvictoria.otero@usc.es